Proceedings World Geothermal Congress 2000
Kyushu - Tohoku, Japan, May 28 - June 10, 2000

FUMAROLE MEASUREMENTS OVER HYDROTHERMAL SYSTEMS

Manfred P.Hochstein[1] and Christopher J.Bromley[2]
[1]Geothermal Institute, The University of Auckland, Priv.Bag 92019, Auckland (NZ)
[2]IGNS, Wairakei, Priv.Bag 2000, Taupo (NZ)

Key Words: fumaroles, steam vents, steam flow rates, heat flow, thermodynamic properties, steam cloud area

ABSTRACT

Methods and theory of fumarole measurements are reviewed and the settings of representative surveys are discussed with reference to some data from the Karapiti fumarole field (NZ) collected during the past 50 years. In almost all cases there is disturbance by some inflow of air which becomes entrained in the turbulent steam jet. Reproducible measurements of the heat output of fumarole jets can be obtained where a jet is funnelled through a vertical pipe or where data are collected across the face of an exposed vent. Systematic errors occur where measurements are made at the ground level of 'crater fumaroles' above a steam vent. The output of inaccessible fumaroles can be estimated from plots of the heat output of accessible fumaroles versus normalised steam cloud area visible in air photos. The last method is suitable for monitoring long term changes in the heat output of fumarole fields occurring over many hydrothermal systems.

1. INTRODUCTION

The term 'fumarole' has been used to describe natural vents discharging dominantly vapour, which turns into wet steam when in contact with air. Fumaroles over volcanic-hydrothermal systems may discharge vapour containing a magmatic gas component. Vents discharging steam without any magmatic gases over hydrothermal systems have also been called 'fumaroles'. Here the term is restricted to fumaroles which discharge steam at temperatures between local boiling and 130 ºC at the surface of hydrothermal systems.

The first measurements of fumaroles of the Tongariro system, New Zealand (NZ), were made in 1937 (Wilson, 1960). Steam cloud characteristics were also used during these early studies to independently assess the total heat output of the fumarole field (Wilson, 1939). The first flow measurements of a large fumarole in the Karapiti area (Wairakei Field, NZ) was reported 50 yr ago (Ledger, 1950). Changes in heat output of this large fumarole field (associated with a liquid dominated system) led to further fumarole studies (Dawson, 1964; Thompson et al., 1964) but the interest in fumarole measurements decreased after 1978. A 1999 re-survey of several fumaroles in the Karapiti area (Hochstein and Bromley, 1999) showed that fumarole measurements can provide reproducible heat output data if the disturbing role of air inflow at the vent can be eliminated or reduced. A review of fumarole measurements is given here to demonstrate that similar studies can be used to assess changes in the natural activity of hydrothermal systems exhibiting fumaroles.

2. PARAMETERS OF AN 'IDEAL' FUMAROLE

Steam flow measurements of a fumarole are introduced in the following with reference to an 'ideal' fumarole as shown in Fig.1. Vapour with a volume flow rate $\Delta V / \Delta t$ (mass flow rate $\Delta m / \Delta t$) escapes as turbulent flow with average speed, v_0, from a vent of cross-sectional area Ao. Some condensation droplets form immediately and a steam jet rises. In the lower part of the cloud, steam rises due to its own momentum which is proportional to the heat output Q. Steam in the upper part of the cloud rises because of its buoyancy which is proportional to $\Delta \rho_m / \rho_{air}$, where $\Delta \rho_m$ is the average density difference of the steam-entrained air mixture in the cloud with respect to the density of ambient air. The volume of the upper cloud reflects its total buoyancy (Scorer, 1958).

Air in the form of a radial inflow with speed u enters the cloud. The steam velocity v in the jet and the air inflow (rate u, maximum u_{max}) decrease with height. Turbulence is enhanced in the annulus surrounding the steam jet. In the centre of the steam jet there is less turbulence which produces a rather flat velocity distribution. The mass flow rate of the air-steam mixture, if measured over an area A' at height z, is therefore always greater than the steam rate at Ao. The setting of the steam jet in Fig.1 already indicates that representative steam flow rates of fumaroles can only be obtained if measurements are made across the whole vent.

3. METHODS AND TECHNIQUES

3.1 Equipment

The volume flow rate of a steam jet is obtained from simultaneous measurements of the dynamic pressure ΔP (Pa) and temperature T (ºC) across the face of the vent with area Ao. The theory of measurements is described in standard texts (for example Massey, 1968).

If a single tube with a short right angle bend at the entrance point (total head tube) is used, the 'stagnation pressure' P can be measured at its exit; it is given by:

$$P = P_0 + \Delta P, \qquad (1)$$

where P_0 is the ambient pressure and ΔP the 'dynamic pressure' caused by the fluid movement at the tip of the probe. A separate measurement of P_0 gives:

$$\Delta P = (1/2)\, \rho_S\, v^2, \qquad (2)$$

where ρ_S is the steam density at temperature T and v the speed of the steam jet. Using two tubes attached together (Pitot tube), of which one is exposed to P_0, the 'dynamic pressure ΔP can be measured directly by using, for example, a U-type manometer filled with a liquid of density ρ_l. The height Δh of the displaced liquid is proportional to ΔP since:

$$\Delta P = \Delta h\, \rho_l\, g\,, \qquad (3)$$

where g is the standard acceleration constant. Water has been commonly used as the liquid. For turbulent flow the head Δh is difficult to measure since rapidly changing velocities in the

jet can propel the water column to anomalous levels. If only (upward) peak readings of Δh are taken, this introduces a systematic error. Liquid manometers tend to give representative readings only for the less disturbed central part of a fumarole.

More reliable readings of P and ΔP can be obtained by using sealed, electronic pressure sensors (SENSYM sensors, for example) whose voltage output varies linearly with P or ΔP. These signals can be displayed in digital form and can be stored for a sequence of readings to yield both mean and standard deviation (S.D.). Such a meter was used recently to re-survey the Karapiti fumarole field (Hochstein and Bromley, 1999). The quick response of modern electronic pressure meters ensures that air-steam flows with occasional reversals in flow direction are always noticed.

Apart from the single 'total head' tube and a standard Pitot tube, a Pitometer, consisting of two modified 'total head' tubes (see, Massey, 1968), can also be used . It measures the difference of forward and opposing ('backward') dynamic pressures, i.e. difference $\Delta P = C\ \Delta P$, where C = 2 for an ideal Pitometer. For the Pitometer we used recently, wind tunnel tests showed that C was c. 1.75. In combination with an electronic pressure meter, a Pitometer can be used to map parts of the jet where rapid changes in flow direction occur. We calibrated all our Pitot tubes in a wind tunnel, since we prefer to use short tubes with larger openings to avoid blockage by condensate or clay particles. The ΔP of a shorter tube can differ (c.1 to 2 %) from that of laboratory type tubes.

3.2 Field setting of fumarole measurements

From a set of ΔP and T data across the face of a fumarole vent, its heat output Q can be obtained since:

$$Q = A_0\ v_{av}\ (\rho_S)\Delta H = (\Delta m / \Delta t)_{av}\ \Delta H \quad (4)$$

where v_{av} and $(\Delta m / \Delta t)_{av}$ are the average speed and mass flow rate of the steam jet respectively; ΔH is the difference in enthalpy of H_S (enthalpy of steam at the observed T) and H_l, the enthalpy of condensation droplets at ambient air temperature. An air inflow component can be reduced if its mass flow rate can be assessed.

Flow measurements of fumaroles have been made in several field settings using different techniques depending on vent accessibility.

(a) The steam jet is restrained by inserting a tube of known cross-sectional area A into the vent and by blocking any escaping steam around the tube. This setting leads to quite accurate measurements of Q.

(b) For larger, accessible vents discharging at moderate speeds (< 50 m/s), measurements of ΔP and T can be made across the vent using a closely spaced grid pattern. The resulting error depends on the degree of air inflow around the vent margin.

(c) Fumaroles surrounded by unstable (thermally altered) ground, but exhibiting an open vent, can be measured using a probe attached to a very long pole. The vibration of the Pitot tube prevents making grid pattern measurements but the centre of the jet, with its characteristic ΔP_{max} and T_{max} values, can be located. With additional single point readings the output Q can be estimated by making appropriate assumptions about u_{max} and v_{av}. This technique has also been used to measure the output of rather small vents, which are not suited for a grid survey.

(d) Fumaroles discharging from an inaccessible vent at the bottom of a crater (surrounded by stable ground) have been assessed by taking measurements at some height z above the vent; the surface level of the crater, for example. These measurements are always disturbed by air inflow. Minimum values of Q can be obtained if areas A and A' (see Fig.1) can be assessed or restrained.

(e) If fumaroles in setting (d) are surrounded by unstable ground, no measurements can be safely made. The majority of large fumaroles in the Karapiti area (Wairakei Geothermal Field, NZ) occur in such an unfavourable setting.

3.3 Fumarole temperatures

The temperature of fumaroles is commonly measured with standard thermocouples (for example, K type). Sharp bends in the thermocouple wire can cause small static shifts of the thermocouple voltage; the same effect can be produced by minor acidic condensates at the soldered tip. All four thermocouples which we used recently gave inaccurate readings (>1 ºC error) near boiling point (B.P.) temperature. Calibrating of thermocouples with respect to B.P. before and after each survey is therefore important. We also used sealed thermistors of small mass. These respond to temperature variations in a steam jet as fast as thermocouples, but without showing static shifts.

More than 20 fumaroles which we have measured during the last 25 years in New Zealand, Java, and Kenya, and which discharged at speeds > 20 m/s, showed T_{max} readings in the centre of the steam jet that were either at local B.P. temperature or greater (up to 130 ºC).

Recent studies (Hochstein and Bromley, 1999) have shown that temperatures in the annulus of a fumarole cloud, i.e. (A'-A) in Fig.1, are always below B.P., exhibiting large standard deviations. Air is therefore always entrained when the temperature, even close to the vent, is below B.P.; hence, the annulus area (A'-A) and the steam jet area A can be assessed from temperature data.

For reliable interpretation of fumarole measurements it is important to know the local boiling temperature which can vary by as much as ± 0.5 ºC due to changes in ambient air pressure P_0. The local B.P. can be inferred from readings of P_0 with reference to saturation temperature (steam tables). The approximate B.P. temperature also can be inferred from the elevation of the fumarole and standard air pressures; it decreases linearly by c. 1 ºC for every increase of 300m in elevation.

4. DISCUSSION OF RESULTS

Fumarole measurements presented here were made in the first four settings listed in 3.2. All examples relate to measurements of fumaroles in the Karapiti area made during the last 50 years. This area is one of the largest fumarole fields in the world associated with a liquid dominated system. Elsewhere at Wairakei, steam is mostly confined by an impermeable layer of mudstone, but at Karapiti a large flow of vapour reaches the surface. Large fumaroles existed in the natural state long before exploitation began in the 1950s. For example, the famous Karapiti Fumarole was active already in 1859. Exploitation of the Wairakei reservoir caused increased boiling at shallow depths, and increased the vapour flux beneath the Karapiti area. A critical assessment of each example of fumarole measurement is given below, to demonstrate the accuracy of measurements and interpretation for each setting.

4.1 Fumaroles discharging through a pipe

The first successful measurement of a large fumarole was made by Ledger in 1950. He restricted the steam flow of the large Karapiti Fumarole, which at that time discharged from the bottom of a c. 1 m deep crater, by a large collector pipe, creating a setting similar to that in Fig.1. The dynamic pressure ΔP at the top of the pipe was sampled with a Pitot tube fixed to a small rail across the top. The temperature at the bottom of the vent was 115.5 ºC, whereas that at the top of the pipe was 116.5 ºC. A U-type mercury manometer was used to infer ΔP; since the tube was filled under water with mercury, the effective density ρ_l in equation (3) was 12590 kg/m3. Using the original data in the report (Ledger, 1950) we found that ΔP_{av} was c. 2.2 kPa; in the centre v_{max} was 71 m/s (2.55 kPa). The original ΔP data and our interpretation are shown in Fig.2.
The mass flow rate of steam through the central part was c. 4.2 kg/s, corresponding to 11 MW heat transfer. Experimental studies (Kays, 1966) show that for fully developed turbulent flow in a circular tube, the average velocity in the annulus (between 0.75 r and r) is c. 0.73 v_{max}, pointing to an output through the annulus of c. 2.7 ± 0.3 kg/s of steam. Allowing for error propagation, the total heat output of the Karapiti fumarole was therefore 18 ± 1 MW. The uncertainty is of the same order (i.e. $\Delta Q/Q < 10$ %) as that of our recent measurements made using encasing pipes, albeit of smaller diameter. Because of errors in the earlier data analysis, mainly due to using an incorrect steam density, Ledger (1950) obtained too low a steam flow rate (c. 5.6 kg/s). The same 'travelling' Pitot tube arrangement was used in 1955 to assess the steam output of the first exploration wells at Wairakei before other techniques (calorimeter and lip pressure method) were developed.

4.2 Grid pattern measurements across an open vent

Some fumaroles discharge horizontally as shown in Fig. 3.1. A large fumarole on the western margin of the Karapiti area (E3 in Hochstein and Bromley, 1999) has a setting similar to that in Fig. 3.1.; it occurs in the same area as an older fumarole (F 714 in Dawson, 1964) which developed from a hydrothermal eruption in 1958. Subsequent widening of the original crater and later blockages led to the development of fumarole E3 in 1997. Because of its easy access we measured the flow of this new fumarole three times between March and May 1999, using both a Pitot tube and a Pitometer; the dynamic pressure was measured with an electronic pressure meter. A thermocouple and a thermistor were used to measure temperature. Although ΔP_{max} and T_{max} varied slightly between surveys, the total heat output was the same, namely 15 MW. Reproducible measurements can therefore be obtained for fumaroles with this setting.
Results of the last survey of fumarole E3 are shown in Fig.3.2. A rectangular grid with spacings of 0.2 m was used; because of natural variations, each ΔP value is the mean of 10 readings taken over c. 1 minute. The area Ao of the vent (c. 0.54 m^2) is outlined by the B.P. temperature contour (local B.P. was between 98.5 and 99 ºC). The maximum velocity of c. 25 m/s occurs in the bottom part of the section where ΔP is 215 Pa; a total mass flow of c. 6.3 kg/s is indicated for Ao. However, around the margin is an area (c. 0.1 m^2) with minor reverse flow, i.e. inflow of an air-steam mixture with T < 98 ºC; the flow direction is dominantly inwards. Assuming an air content of 50%, a maximum mass flow of c. 0.6 kg/s is indicated for the inflow, which reduces the actual steam outflow to c. 5.7 kg/s, corresponding to c. 15 MW of heat output. Assumptions made about the air-steam inflow therefore limits the accuracy of such a survey. The total uncertainty of 1.5 MW (i.e. $\Delta Q/Q = 10\%$) is given by the difference of the means of all three surveys.

4.3 Single point measurements in an open vent

The flow rate of fumaroles in the same setting as that shown in Fig.3.1, but discharging at higher speeds, can often only be assessed from 'single point' measurements of ΔP_{max} and T_{max} taken in the centre of the jet, since the movement of the tip of the pressure tube allows no grid survey. The same problem arises where measurements must be made with a long extension of the tube where the ground is unstable. Powerful fumaroles in the Ketetahi area (Mt Tongariro, NZ) were assessed by such 'single point' surveys (Walsh et al., 1998). We used the same method recently to assess the output of several fumaroles in the northern part of the Karapiti area which all discharge laterally from open vents.
Results from one of the northern fumaroles are shown in Fig.3.3. In the centre of the jet, ΔP_{max} was 4.16 kPa and T_{max} was 112 ºC, pointing to a maximum speed v_{max} of almost 100 m/s. The maximum speed of the inflow (u_{max}) at the top was also large, of the order of c. 40 m/s, thus confirming the assumption made in Fig.1 that the magnitude of u is proportional to that of the steam outflow. Using an empirical relationship between v_{av} and v_{max} (Hochstein and Bromley, 1999), and assuming that $0.6 < (v_{av} / v_{max}) < 0.7$, an average speed of 60 to 70 m/s was inferred for the vent in Fig.3.3. Allowing for the air inflow component, a net steam flow rate of c. 0.9 to 1.7 kg/s is indicated. The likely output of fumarole B3 lies between c. 2.4 and 4.5 MW with a resultant error of the mean of c. 30 %.

4.4 Measurements of steaming pits and craters

Fumaroles in thermally altered ground usually start with a steam eruption creating a deep pit; partial blockage of the vent at the bottom causes further steam eruptions which deepen the crater until some final blockage occurs. The setting of such a 'crater fumarole' is shown in Fig. 4.1. Measurements of the apparent steam flow of steaming pits and craters in the Karapiti area were reported at the first International Geothermal Congress (1961) in Rome (Thompson et al., 1964).
Our recent attempt to measure the steam flow of a steaming pit in the setting of Fig. 4.1 showed that vigorous air inflow increases the total mass flow rate to several times that coming from the steam vent if measurements are made at the surface of such a crater (Hochstein and Bromley, 1999). The true steam flow rate was obtained when the original discharge area A', exhibiting steam-air mixture temperatures between 96 and 97 ºC over most of the crater, was reduced until the temperature of the jet was at boiling temperature throughout the reduced area A (c. 0.1 A'). We had observed a similar effect during some of our earlier studies in Indonesia.

Our recent survey casts doubt upon some earlier fumarole measurements made in the Karapiti area in the setting shown in Fig. 4.1. In the earlier studies ‘peak values’ of the dynamic pressure ΔP were recorded with a U-type water manometer over the whole crater area A". Only contoured 'apparent heat flow' values were published, pointing, for

example, to a large apparent heat output of c. 30 MW (Dawson, 1964) of the crater fumarole F 714, the parent fumarole in the area which now hosts the new fumarole E3 (see 4.2).
To re-interpret the 1960 survey, we re-compiled the original data, as shown in Fig. 4.2. It can be inferred that pure steam is only transferred through the inner part (A) of the jet, as outlined by temperatures greater than B.P. (c.98.5 ºC), whereas downflows (and upflows) of a heated air-steam mixture are dominant in the outer area. Another problem is indicated by the geometry of the steam jet and that of area A, as shown in the inset of Fig. 4.2. We adopted the reduction as used by Dawson (1964) by projecting the area A onto an area normal to the direction of the steam jet (i.e. Ao), neglecting geometric spreading. Using the mean ΔP values as shown in Fig.4.2, a minimum output of c. 13 MW is indicated for all steam passing through area A. Some steam, however, is also transferred through the (shaded) annulus (A'-A). Any assessment of that component depends upon the assumption of the air-steam ratio in the annulus. If the steam component was c. 30%, as found recently for another steaming crater in the same area (fumarole I1, described by Hochstein and Bromley, 1999), the total discharge of F 714 would increase by c. 3.5 MW. The total output of F 714, however, would have been significantly less than the 30 MW quoted in 1964. Measurements of the steam output of crater fumaroles at the lip of the crater are therefore not reliable, unless the steam from the deep vent can be funnelled through a pipe or the total discharge area A at the surface can be reduced to that of Ao.

5. STEAM CLOUD VOLUME AND HEAT OUTPUT

If only the output of fumaroles with accessible, open vents can be measured, the question arises whether the output of the inaccessible fumaroles of a large fumarole field, such as Karapiti, can be assessed. During earlier surveys (for example, Thompson et al., 1964) it was assumed that there is a clear proportionality between the volume of steam clouds over adjacent fumaroles and their heat output. Since cloud volumes are difficult to measure, it was further assumed that the projection of a steam cloud onto the ground, visible, for example, in a vertical air photo, is also proportional to its volume. No clear proof of these assumptions is given in the earlier studies.
Steam in the lower part of a fumarole cloud rises due to the momentum of the jet, and in the upper part due to buoyancy; both parameters are proportional to the heat output. A steam cloud volume is also a function of numerous meteorological parameters, such as air temperature, air pressure, humidity, wind speed, exposure to radiation, etc. Empirical multi-parameter relations between the volume of a single, buoyant steam cloud and heat output have been developed (cited in Kagiyama, 1981), but these could not be applied to the fumarole clouds in the Karapiti area since most of the meteorological parameters were not recorded. A non-dimensional parameter approach was therefore indicated.
We have used the ratio of a single steam cloud area Ai and the total steam cloud area (ΣA) over a whole fumarole field as such a non-dimensional parameter (Hochstein and Bromley, 1999). The two areas were assessed from the opaque part of steam clouds visible in a set of air photos taken over the Karapiti area in 1997 and 1998. It was found that there is indeed a quasi-linear relation between log ΔQi and log Δ(Ai / ΣA) for all fumaroles in the Karapiti area which we surveyed between March and May 1999. A log-log plot is shown in Fig.5; the intersection of the best fit line with (ΣAi / ΣA) gives the heat output for all fumaroles in the Karapiti area, namely c. 80 MW. Since the output of all measured fumaroles was c. 25 MW, that of all others was therefore c. 55 MW.
The same method, albeit using a smaller number of 'calibrated' fumaroles, has been used to assess the total output (c. 37 MW) of all fumaroles in the greater Olkaria area (Hochstein and Kagiri, 1997). The relationship shown in Fig.5 appears therefore to be valid for other fumarole fields associated with hydrothermal reservoirs.

6. CONCLUSIONS

Methods and settings of fumarole measurements have been reviewed. It has been shown that reproducible heat output data of accessible fumaroles can be obtained if the dynamic pressure ΔP and the temperature T of a steam jet are mapped across the whole open vent. Systematic errors occur if the disturbing inflow of heated air at the margin of the vent is not recognised. The speed of inflowing air appears to be proportional to that of the jet. Such inflow is indicated by the flow direction and flow pulsations if ΔP values are measured with modern electronic pressure meters. Air entrainment cannot be recognised from the visual appearance of the steam jet. The effective cross-sectional area of a turbulent steam jet can be determined by making closely spaced temperature measurements; temperatures in the jet are always at or above the local boiling temperature. Significant air entrainment is already indicated if temperatures at the jet margin are a few degrees below boiling.
The most reliable measurements of the output Q are those made where the steam jet is funnelled through a pipe to become fully turbulent at the pipe exit (ΔQ/Q < 10 %). Quite accurate measurements can also be obtained if multiple measurements are taken across an exposed steam vent, especially if steam is discharged laterally (c. 10% uncertainty for ΔQ/Q). Inaccurate results are obtained if measurements are made at the lip (i.e. ground level) of 'crater fumaroles'; the mass flow rate of heated air which enters the crater and is expelled through a wide annulus usually exceeds the steam flow rate. In this setting the uncertainty ΔQ/Q is always >> 30 %. Most of the published earlier measurements in the Karapiti area were from crater fumaroles.
The output of inaccessible fumaroles can be assessed from a plot of the heat output of measured fumaroles versus the ratio of their steam cloud areas, normalised with respect to the total steam cloud area of the whole fumarole field. This indicates a quasi-linear relationship between the two, in the case of the Karapiti area. The same relationship has been used to assess the output of all fumaroles over the Olkaria Field in Kenya.
Since the total heat output of a fumarole field can be obtained from measurements made of a few accessible fumaroles, secular changes in the overall output caused, for example, by exploitation or long term climatic changes can therefore be assessed to provide data for reservoir management and environmental monitoring.

ACKNOWLEDGEMENTS

We thank Dr M. Sorey for the loan of a digital pressuremeter and pitometer, Mr D Hamilton, Mr Duncan Graham, and Mr Dave Keen for assistance with wind tunnel and field measurements, and NZ Foundation for Research Science and Technology (CO5605) for some funding assistance. Ms L. Cotterall is thanked for her help with drafting.

REFERENCES

Dawson, G.B. (1964). The nature and assessment of heat flow from hydrothermal areas. *NZ Jnl. of Geology and Geophysics*, 7, pp.155-171.

Hochstein, M.P. and Kagiri, D. (1997). The role of 'Steaming Ground' over high temperature systems in the Kenya Rift. *Proc. 22nd Workshop on Geothermal Reservoir Engineering,* Stanford University, pp. 29-35.

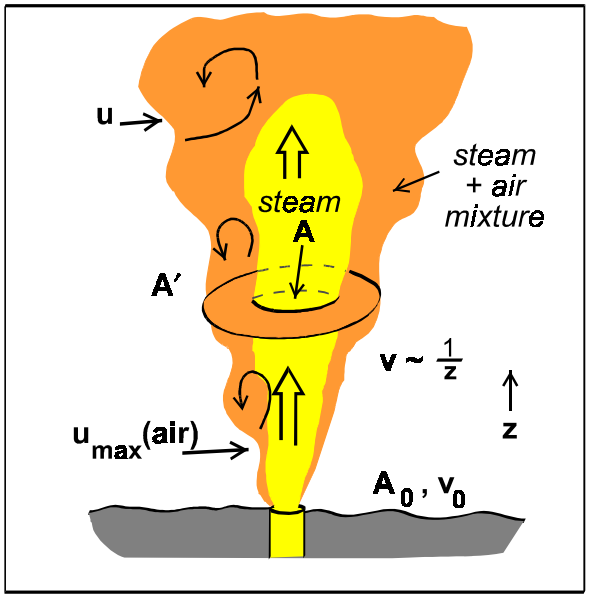

Fig. 1. Parameters of an 'ideal' fumarole.

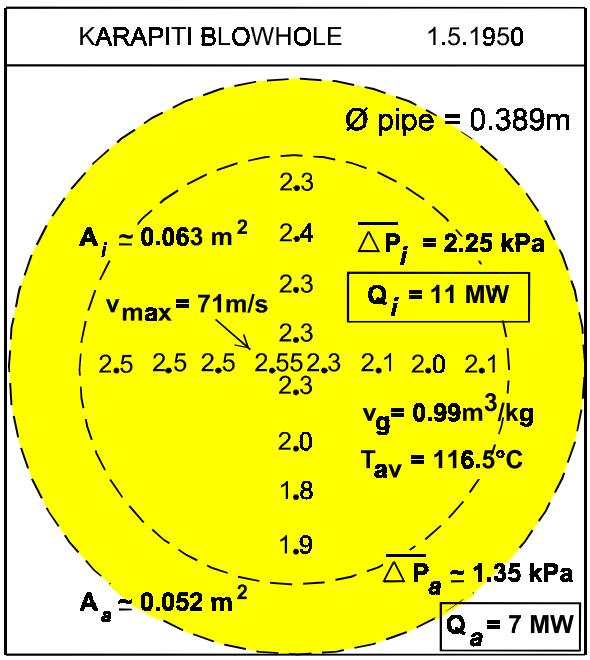

Fig. 2. Dynamic pressure (ΔP) in kPa across a vertical pipe funneling the Karapiti Blowhole fumarole (1950 data).

Hochstein, M.P. and Bromley, C.J. (1999). Recent fumarole measurements in the Karapiti Area ('Craters of the Moon'), Wairakei Field, New Zealand. *Proc. 21st NZ Geothermal Workshop*, Univ. of Auckland, pp. 15-20.

Kagiyama, T. (1981). Evaluation methods of heat discharge and their application to the major active volcanoes in Japan. *Jnl. of Volcanology & Geothermal Research*, 9, pp. 87-97.

Kays, W.M. (1966). *Convective Heat and Mass Transfer*. McGraw-Hill, New York. 387 pp.

Ledger, R.L. (1950). *Measurement of steam flow from Karapiti Blowhole*. Report for Dominion Laboratory, DSIR, Wellington. 6 pp.

Massey, B.S. (1968). *Mechanics of Fluids*. Van Norstrand Co Ltd, London. 508 pp.

Scorer, R.S. (1958). *Natural Aerodynamics*. Pergamon Press, London. 312 pp.

Thompson, G.E.K., Banwell, C., Dawson, G., Dickinson, D.J. (1964). Prospecting of hydrothermal areas by surface thermal surveys. *Proc. UN Conference on New Sources of Energy (Rome, 1961)*, Vol.2, UN New York. pp.386-401.

Walsh, F.D., Hochstein, M.P., and Bromley, C.J. (1998). The Tongariro geothermal system (NZ): Review of geophysical data. *Proc. 20th NZ Geothermal Workshop*, Univ. of Auckland, pp. 317-324.

Wilson, S.H. (1939). Measurement of the amount of steam escaping from areas of volcanic or solfataric activity. *Nature*, 143, pp. 802-803.

Wilson, S.H. (1960). Physical and chemical investigation of Ketetahi Hot Springs. In: *The Geology of Tongariro Subdivision*, D.R.Gregg (Ed). NZ Geological Survey Bulletin 40, Wellington. pp. 124-144.

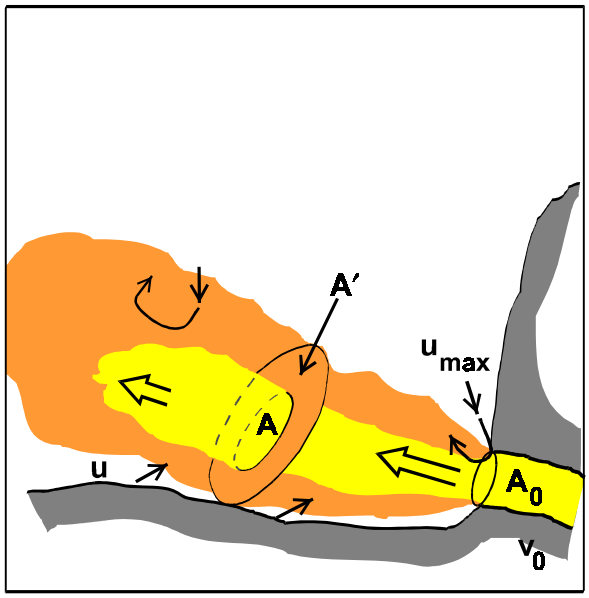

Fig. 3.1. Fumarole with lateral discharge.

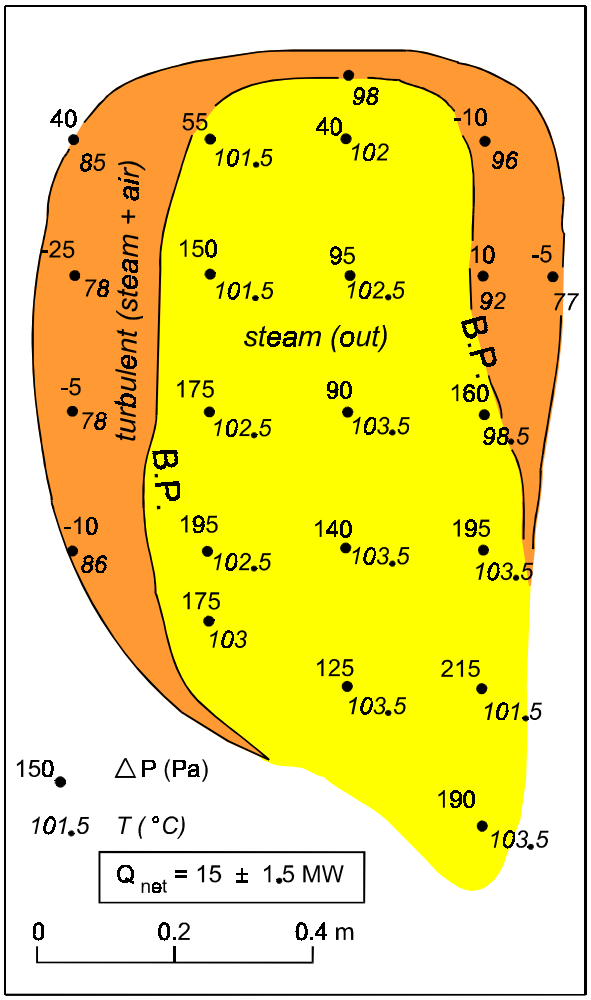

Fig. 3.2. Grid pattern measurements of dynamic pressure (ΔP) in Pa and temperature (T) across open vent of fumarole E3 (Karapiti; 1999 data).

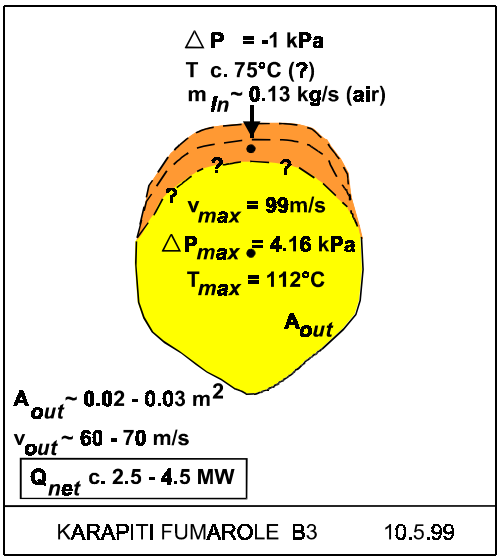

Fig. 3.3. Single point measurements in open vent of fumarole B3 (Karapiti; 1999 data).

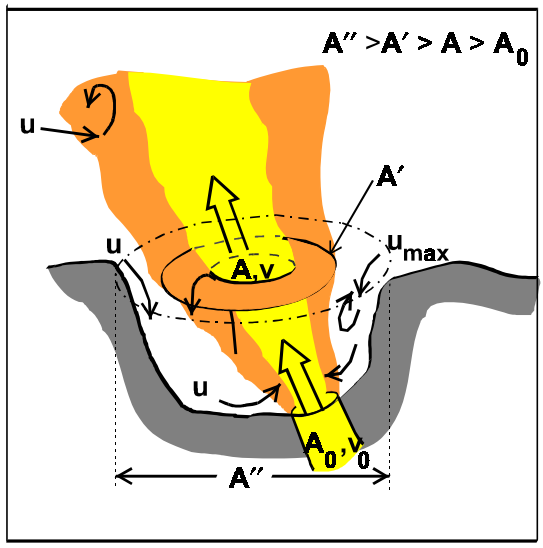

Fig. 4.1. Fumarole discharging from the bottom of a steaming crater.

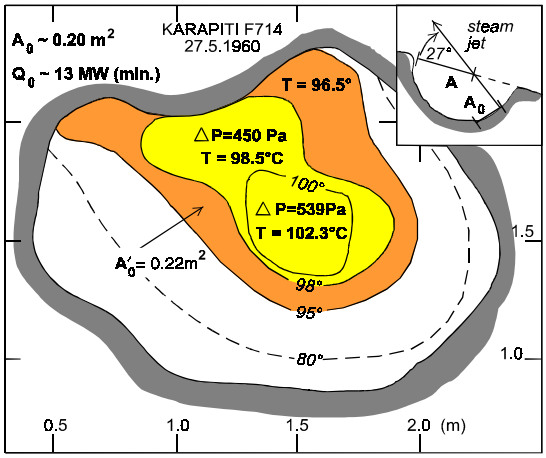

Fig. 4.2. Dynamic pressures (avg) and temperatures (contours) across the crater fumarole F 714 (Karapiti; 1960 data).

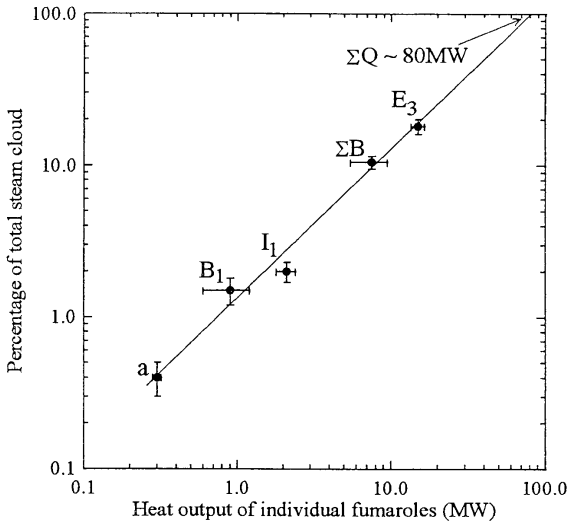

Fig.5. Heat output (1999 data) versus normalised fumarole cloud area of the Karapiti fumarole field.